Annales Societatis Geologorum Poloniae (2023), vol. 93: 467–481 https://doi.org/10.14241/asgp.2023.15

CORROSION OF CARBONATE SPELEOTHEMS BY AN ALLOGENIC RIVER INFERRED FROM PETROGRAPHY AND A WEIGHT LOSS EXPERIMENT: A CASE STUDY FROM THE DEMÄNOVÁ CAVE SYSTEM, SLOVAKIA

Przemysław SALA[1*] & Pavel BELLA[2, 3]

[1] *Institute of Geological Sciences, Jagiellonian University, Gronostajowa 3a, 30-387 Kraków, Poland; e-mail: p.sala@uj.edu.pl*
[2] *Department of Geography, Faculty of Education, Catholic University in Ružomberok, Hrabovská cesta 1, 031 04 Ružomberok, Slovakia*
[3] *State Nature Conservancy of the Slovak Republic, Slovak Caves Administration, Hodžova 11, 031 01 Liptovský Mikuláš, Slovakia; e-mail: pavel.bella@ssj.sk*
** Corresponding author*

Sala, P. & Bella, P., 2023. Corrosion of carbonate speleothems by an allogenic river inferred from petrography and a weight loss experiment: a case study from the Demänová Cave System, Slovakia. *Annales Societatis Geologorum Poloniae*, 93: 467–481.

Abstract: The crystallization of speleothems can be interrupted by the invasion of allogenic water into cave passages. These interruptions were studied, both in speleothems currently submerged in an underground river and in speleothem sections, which were found at the lowermost fluvially active passage level of the Demänová Cave System. The interaction between speleothems and allogenic water, undersaturated with respect to calcite, is manifested in the presence of siliciclastic material and the corrosion of calcite crystals. The progressive development of corrosion features depends on the duration of the interaction of calcite crystals with allogenic water. Moreover, the movement of the water and siliciclastic deposition over the speleothems can influence the corrosion process. The estimated rate of corrosion, caused by the underground Demänovka River and measured by the weight loss of experimental tablets, is up to 0.029 mm/y. U-series dating indicated that the interaction of speleothems with allogenic water occurred during the Vistulian (Weichselian). The identification of corrosion episodes, caused by allogenic water, is a step towards understanding the origin of hiatuses and establishing criteria for recognition of them.

Key words: Karst, carbonates, hiatus, dissolution, palaeoenvironment.

Manuscript received 6 May 2023, accepted 27 July 2023

INTRODUCTION

Speleothems have been employed broadly in palaeoenvironmental reconstruction during the last thirty years. Speleothem-based studies have been performed in various geographic regions, except for the polar zones. A robust application of speleothems is provided by the precise determination of their crystallization age, which can be tied to various proxies that record past environmental conditions (e.g., Bar-Matthews *et al.*, 1997, 2010; Burns *et al.*, 2001; Cruz *et al.*, 2005, 2007; Spötl *et al.*, 2006; Fairchild and Baker, 2012; Warken *et al.*, 2018; Błaszczyk and Hercman, 2022; Bernal-Wormull *et al.*, 2023).

Studies of speleothems revealed that their crystallization is commonly punctuated by hiatuses (e.g., Frumkin *et al.*, 1999; Hercman, 2000; Bosák *et al.*, 2002; Plagnes *et al.*, 2002; Railsback *et al.*, 2013; Pawlak *et al.*, 2020; Sierpień *et al.*, 2021; Zupan Hajna *et al.*, 2021). These result from various processes, including the reduction or absence of a supply of drip water (e.g., Moreno *et al.*, 2010; Railsback *et al.*, 2013), dissolution (corrosion) by water undersaturated with respect to calcite (e.g., Railsback *et al.*, 1994, 2013; Perrin *et al.*, 2014; Martín-Chivelet *et al.*, 2017), the deposition of non-carbonate material (e.g., Gázquez *et al.*, 2014; González-Lemos *et al.*, 2015a, b) or the mechanical destruction of the speleothems (e.g., Kagan *et al.*, 2005; Szczygieł *et al.*, 2021; Sala *et al.*, 2022). The dissolution of speleothems is commonly linked to the presence of aggressive

drip water. However, their dissolution also can be expected where there has been the invasion of floodwater into already drained cave segments that are occupied by speleothems (Palmer, 2001; Hercman *et al.*, 2008). Additionally, floodwaters usually carry a significant quantity of detrital particles that can be deposited on speleothems, resulting in an interruption in their growth. The detrital layers, incorporated into speleothems, were studied with regard to flood frequency and their timing (e.g., Dorale *et al.*, 2005; Dasgupta *et al.*, 2010; Quigley *et al.*, 2010; Finné *et al.*, 2014; Denniston and Luetscher, 2017). These detrital layers are commonly recognized through standard petrographic observations, but advanced analytical methods, including XRF scanning (Finné *et al.*, 2015) and palaeomagnetic techniques (Feinberg *et al.*, 2020; Sánchez-Moreno *et al.*, 2022), also have been applied. Yet only minor insights have been gained into the petrographic features of the corrosion of speleothems caused by floodwater (González-Lemos *et al.*, 2015b; Denniston and Luetscher, 2017).

Speleothems, occurring at the lowermost level of the Demänová Cave System (DCS), are intercalated with siliciclastic sediments that were deposited by an allogenic underground river (Bella *et al.*, 2021). In this study, the present authors aimed to identify the corrosion features of speleothems, caused by aggressive river water, and attempted to estimate the rate of corrosion by applying the rock tablet method. Corrosion features, developed on the speleothem surface, currently submerged in an underground river were compared with their fossil analogues, recognized in the speleothems flooded in the past. On this basis, the authors propose that the identification of corrosion features can be used for the detection of cave flood episodes, recorded in the speleothems, and provides insights into karst palaeohydrology.

GEOLOGICAL AND SPELEOLOGICAL SETTING

The DCS is located in the northern part of the Low Tatra Mts, which occupy the central-north part of Slovakia. The DCS developed in the Middle Triassic (Anisian–Ladinian) carbonate rocks, mostly dolomites and limestones of the Gutenstein-type and dolomites of the Ramsau-type (Fig. 1A; Droppa, 1972; Gaál, 2016; Gaál and Michalík, 2017). These rocks belong to the Krížna Nappe, thrust over the crystalline granitoid core of the Low Tatra Mts (Biely *et al.*, 1992). Glacial tills, reported in the upper part of the Demänová Valley, indicate its glaciation during the late Middle and Late Pleistocene periods (Vitásek, 1923; Louček *et al.*, 1960; Droppa, 1972).

The DCS is the most extensive cave system in Slovakia, reaching in excess of 43 km, and consisting of several evolution levels that correspond to successive stages in the incision of the nearby Demänová Valley (e.g., Droppa, 1966, 1972; Bella *et al.*, 2014; Hercman *et al.*, 2023). The lowermost level of the DCS is occupied by an active underground branch of the Demänovka River. At several locations the underground river deposited thick sequences of siliciclastic sediments. One of them is present on the eastern river

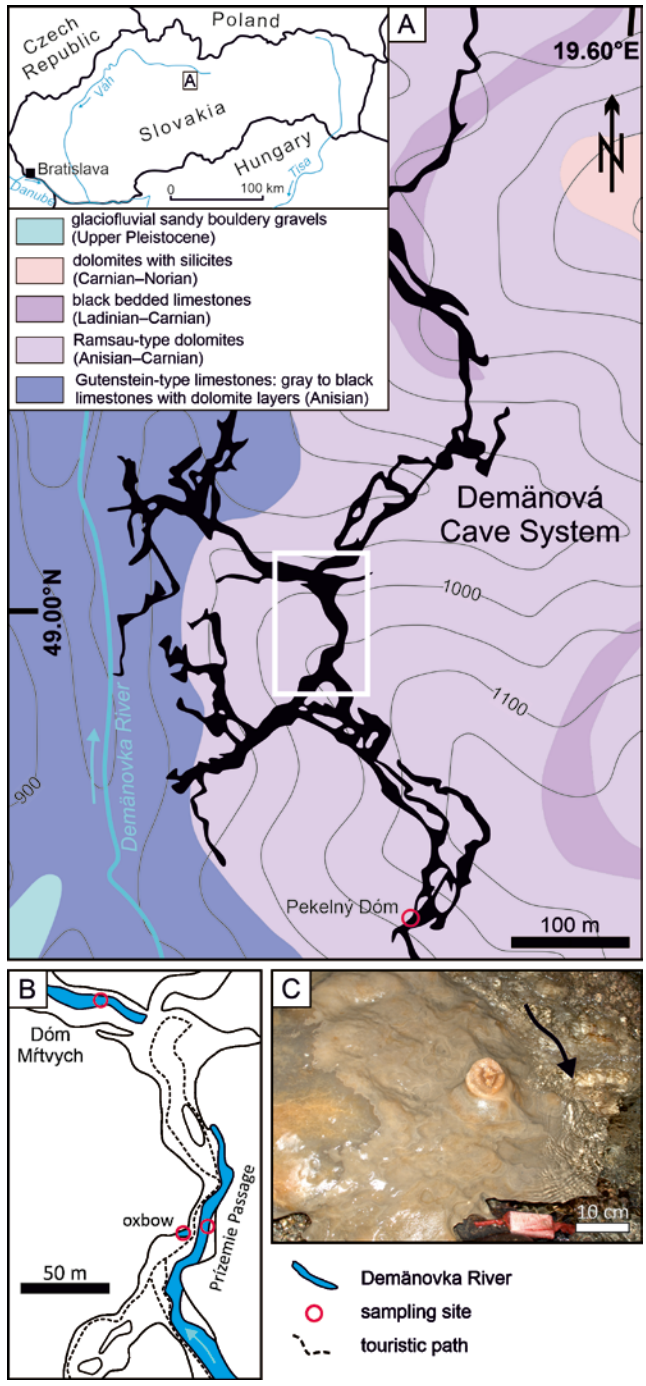

Fig. 1. Localization and speleological setting. **A.** Geological setting of the DCS (based on Biely *et al.*, 1992). **B.** Sketch of the studied part of the DCS (redrawn from Droppa, 1957). **C.** Flowstone in the Prízemie Passage submerged in the Demänovka River. Note the speleothem tablet bathed in water. Arrow indicates the direction of water flow.

bank in the Prízemie Passage (Fig. 1B; see also Bella *et al.*, 2021). These deposits contain numerous speleothems, mostly flowstones, which are sandwiched between the siliciclastic sediments. Owing to the dissection of these sediments by the river, flowstone blocks slid on to the riverbed (Fig. 1C). In the Prízemie Passage, on the western side of the underground river, there is a small oxbow with ponding water. In the Pekelný Dóm Chamber, located ca 500 m upstream from

the Prízemie Passage, the speleothem false floor was identified approximately 4 m above the present riverbed.

The Demänová Valley is drained mainly by the allogenic Demänovka River, which flows from the non-karstic area, located south of the DCS. The discharge of the river ranges from 0.1 to 0.9 m^3/s, while its peaks occur during May and June–July, owing to melting of snow cover and intense summer precipitation (Bella *et al.*, 2014). Entering the karst area, the river bifurcates and a branch flows underground. The underground river carries the water of Ca-Mg-HCO_3 type, while its average calcite saturation index is –0.42 (Motyka *et al.*, 2005; Haviarová *et al*., 2021).

MATERIAL AND METHODS

Water analyses

Pilot water samples were collected for chemical analysis from an underground section of the Demänovka River and the oxbow in the Prízemie Passage. The concentrations of major ions (Ca^{+2}, Mg^{+2}, Na^{+}, K^{+}, HCO_3^{-}, SO_4^{-2}, Cl^{-}) were determined in seven water samples, using a DIONEX ICS-2000 gas chromatograph with an AS-40 autosampler. The pH and EC of the water were measured, using a WTW pH/Cond 3320 portable multimetre with a Sentix41 pH probe and TetraCon425 probe, respectively. Calculations of the calcite saturation index (SI_{calc}) of the water were performed, using the PHREEQC program (Parkhurst and Apello, 2013).

Tablets corrosion experiment

The corrosion rate of speleothems by the allogenic river was obtained by the tablet method (see Krklec *et al.*, 2021). The tablets were made of finely laminated and slightly porous calcite flowstone, which was collected during the excavation of Zygmunta Cave, located in the Kraków-Częstochowa Upland. The size of these tables was approximately 8 x 4.2 cm. The tablets were cut but not polished to keep their original roughness and to prevent the resulting powder from filling the pores. Before deployment, the tablets were rinsed under running water, dried at 60°C for 48 hours, and weighed with an accuracy of 0.001 g. Twelve tablets were inserted into a nylon net and rigidly attached by plastic wire to rock blocks on their downstream sides and submerged in the underground river in the Dóm Mŕtvych Chamber and the Prízemie Passage (Fig. 1B, C). Additionally, three tablets were placed in the stagnant water filling the oxbow in the Prízemie Passage. All the tablets were exposed to interactions with the water for 908 days. After this time, the tablets were carefully transported to the laboratory, where they were processed (rinsing, drying, and weighting) in the same manner as before deployment. The difference in weight was calculated in mm/y relative to the surface of each tablet, with the calcium carbonate density accepted as 2.71 g/cm^3 (see Krklec *et al.*, 2021).

Speleothems

Speleothem sampling in the DCS was limited to the Prízemie Passage and was kept to a minimum through attention to conservation. Samples were collected directly from the Demänovka River and from the section of siliciclastic deposits. The former included the flowstones DMV1, S1 and S10, which served for the observations of the corroded surfaces (Tab. 1). Sample DMV1 was taken from the large flowstone block that had slid into the river (Fig. 1C). The material for analysis of surface of the speleothems was supplemented by flowstones RA1 and RA10 that were sandwiched in the section of siliciclastic deposits. The aforementioned samples (DMV1 and RA10), but also the DMV5 flowstone sample, which was taken from the section of the siliciclastic deposits, are assumed to record the hiatuses associated with the corrosion of speleothems by the allogenic river (Tab. 1). The studied material was supplemented by the PD4 stalagmite in the Pekelný Dóm Chamber that grew ca 4 m above the recent level of the underground Demänovka River. This stalagmite was previously studied in the context of palaeoenvironmental reconstruction (Podgórska, 2019) and an age estimate for the depositional break (Pawlak *et al.*, 2020).

Table 1

Corrosion surfaces and hiatuses analysed in the speleothem samples.

Sample no.	Corrosion surface	Corrosion hiatus
DMV1	+	+
DMV5		+
PD4		+
RA1	+	
RA10	+	+
S1	+	
S10	+	

Analytical methods

All the studied speleothems and experimental tablets were examined for the presence of corrosion traces and incorporated siliciclastic material. This was accomplished by means of a standard optical microscope, using thin sections, while their preparation was preceded by hardening of the samples with epoxy resin. The speleothem and tablets surfaces were also investigated, using a scanning electron microscope coupled with an energy dispersive spectrometer (SEM-EDS). All the specimens examined with the SEM previously had been coated with carbon. The terminology applied in the description of calcite fabrics in this study was adapted from Frisia (2015).

The mineral composition was determined, using the X-ray diffraction method (XRD). Four samples were drilled from the interiors of the speleothems, while two additional samples were collected from the surfaces of the experimental tablets. Measurements were made with a Philips X'Pert APD diffractometer with CuKα radiation and operating in the angle range of 2–70°.

Some hiatuses present within the speleothem sections were analysed for element distribution using, the electron probe microanalysis (EMPA). A set of elements (Ca, Mg, Si, K, and P) was mapped on the polished thin sections, coated with carbon. The analyses were done by means of the JEOL SuperProbe JXA-8230 at the Laboratory of Critical Elements of the AGH University of Science and Technology, KGHM Polska Miedź S.A. The device is equipped with six wavelength dispersive spectrometers, utilizing synthetic analyser crystals: PETJ, PETH, LiF, LiFH, TAP, and TAPH. The system operated in a wavelength-dispersive (WDS) mode under the following conditions: an accelerated voltage of 15 kV, beam current of 15 nA, beam size of 1–5 μm, peak count time of approximately 20 s, and a background time of 10 s.

DMV1 and DMV5 flowstones that displayed growth hiatuses, resulting from the deposition of siliciclastic material, were drilled for U-series dating. Samples were taken from the dense calcite layers, approximately 0.2 mm below and above the hiatuses. The thickness of the samples was kept to a minimum and their mass did not exceed 0.3 g. Firstly, the samples were treated at high temperatures (800°C, over 6 hours) to decompose any organic matter, then they were dissolved in nitric acid, and subsequently uranium and thorium were separated from the carbonate matrix by the chromatographic method, using TRU Resin (Hellstrom, 2003). The above-mentioned steps were completed at the U-series Laboratory of the Institute of Geological Sciences, Polish Academy of Sciences (Warsaw, Poland). Secondly, the measurements of U and Th isotopic compositions in all the samples and standards were performed at the Institute of Geology of the Czech Academy of Sciences (Prague, Czech Republic) using a double-focusing sector-field ICP mass analyzer (Element 2, Thermo Finnigan MAT). The instrument was set on a low mass resolution ($m/\Delta m \geq 300$). U-series ages were calculated from measured $^{230}Th/^{234}U$ and $^{234}U/^{238}U$ activity ratios. All uncertainties, except for the decay constant uncertainties, were evaluated and taken into account, when assessing the age uncertainty, using error propagation rules. The ages obtained for samples with $^{230}Th/^{232}Th$ activity ratios below 300 (Hellstrom, 2006) were adjusted for detrital contamination, indicated by the presence of ^{232}Th, using typical silicate activity ratios (e.g., Cruz *et al.*, 2005).

RESULTS

Water analyses

The chemical analyses of the underground Demänovka River showed that the pH of the water is approximately 7.55 and the electroconductivity (SEC) values range between 218 and 230 μS/cm (Tab. 2). The dominant cations in these waters are Ca^{+2} and Mg^{+2}, while anions are represented mainly by HCO_3^- and SO_4^{-2}. The concentration of other ions is minor. The calculated SI_{calc} values of the river water range from –0.92 to –0.69. The average pH value of the oxbow water is 7.68. Moreover, the SEC values of the former were between 317 and 335 μS/cm. Like the river water, those in the oxbow show the highest concentration of Ca^{+2} and Mg^{+2} among cations, while anions are dominated by HCO_3^- the average value of which was 138.1 mg/l. The SI_{calc} values of the oxbow water are between –0.47 and –0.37.

Tablet corrosion experiment

The weight loss of the tablets, exposed to interaction with the undersaturated cave waters, ranged from 0.042 to 1.223 g (Tab. 3). This is equivalent to a range of between 0.001 and 0.029 mm/y. A significantly higher weight loss was observed for the tablets, installed in the river, than for those placed in the stagnant water of the oxbow. The average weight loss of the former was 0.986 g (0.022 mm/y), with a standard deviation equal to 0.134 g (Tab. 3). In contrast, the average weight loss of the tablets placed in the oxbow was 0.054 g (0.001 mm/y), with a standard deviation of 0.013 g.

The experimental tablets were composed of calcite that mainly exhibits a dendritic fabric. The tablets, exposed to the interaction with the river water, have more irregular and rough surfaces relative to their original microtopography (Fig. 2). The dissolution of the tablets is expressed by the presence of numerous corrosion pits within the calcite crystals (Fig. 3A–C). These corrosion pits usually have trench-like forms, frequently with jagged crystal faces. The diameters and depths of these pits usually do not exceed tens of micrometres. Tablets placed in the oxbow with stagnant water showed only minor dissolution features (Fig. 3D).

Table 2

Major ion concentration and saturation indices (SI_{calc}) of the studied water samples. Standard deviations are given in the brackets.

Sampling site	pH	SEC	Ca^{+2}	Mg^{+2}	Na^+	K^+	HCO_3^-	SO_4^{-2}	Cl^-	NO_3^-	SI_{calc}	Error
		μS/cm	mg/l									(%)
River (n = 4)	7.55 (0.08)	219 (5.8)	28.14 (6.76)	8.90 (6.36)	1.53 (0.58)	0.53 (0.12)	89.30 (10.56)	26.64 (10.01)	1.43 (0.30)	4.19 (1.30)	–0.84 (0.11)	2.2 (3.0)
Oxbow (n = 3)	7.68 (0.12)	324 (9.9)	35.28 (4.81)	16.59 (4.29)	1.12 (0.59)	0.48 (0.16)	138.06 (12.21)	15.95 (7.77)	1.45 (0.45)	(5.52) (1.25)	–0.42 (0.05)	–0.4 (5.7)

These are represented by thin and elongated trench-like pits, micrometres in diameter, that developed along the calcite crystal faces. It should be stressed here that some larger deviations in the microtopography of the tablets, especially those placed in the oxbow, could have resulted from original differences in crystal morphology or their possible damage during tablet preparation.

Speleothem surfaces

The flowstones studied were composed of calcite. Corrosion of their surfaces by the underground river is displayed in various macroforms. Some of the surfaces show the presence of scallops, up to 5 cm long (Fig. 4A). Their depth usually does not exceed 1 cm. Within the scallops, small corrosion pits, commonly less than 1 mm in diameter, were observed (Fig. 4B). On the other hand, the corrosion is manifested by shallow depressions of different sizes and shapes that are irregularly distributed on the speleothem surface (Fig. 4C). These depressions result from the truncation of the uppermost layers of the speleothems and are usually up to a few millimetres deep (Fig. 4D, E).

Calcite crystals, observed below the corroded speleothem surfaces, show the presence of corrosion pits, which usually are developed at the junctions with neighbouring crystals (Fig. 5A, B). These corrosion pits have elongated or quasi-oval cross-sections. The individual corrosion pits have a diameter that commonly does not exceed 50 μm. However, many of them are interconnected, resulting in an enlargement in size. The depth of the corrosion pits varies between less than 10 and up to 100 μm. The faces of corroded calcite crystals are rough and show the presence of small and numerous corrosion pits that lead to the development of an openwork structure within the crystal (Fig. 5C). The calcite crystals affected by the underground river also show the presence of well-rounded to almost flat terminations (Fig. 5D, E). It should be noted that the calcite crystals, which were covered by siliciclastic sediments, avoided significant dissolution. In such cases, the terminations usually retain their original shape, while their faces are flat and free from corrosion pits (Fig. 5F).

Hiatuses within speleothem sections

The studied speleothems are in the majority composed of calcite, while aragonite was detected only subordinately. The calcite crystals below the hiatuses are mainly represented by columnar and columnar elongated fabrics. Differences in the preservation state of the calcite crystals was observed, depending on the sample. The crystals affected by corrosion commonly showed the presence of numerous corrosion pits of various diameters (Fig. 6A, B). Their depths usually did not exceed 50 μm; however, occasionally corrosion pits up to 200 μm deep were noted. It is noteworthy that these pits were commonly observed at the junctions with neighbouring calcite crystals. The terminations of the corroded calcite

Table 3

Corrosion rate of speleothem tablets exposed to interaction with water for 908 days.

Sample no.	Weight loss [g]	Surface [cm^2]	Corrosion rate [mm/y]
River			
10	1.139	66.33	0.0256
11	1.223	63.52	0.0287
12	0.899	69.46	0.0193
13	0.827	70.13	0.0176
15	1.005	64.08	0.0233
16	0.923	67.90	0.0202
17	1.115	65.97	0.0252
19	0.946	66.34	0.0212
20	0.870	65.51	0.0198
23	0.855	66.04	0.0193
24	0.957	64.44	0.0221
25	1.077	67.84	0.0236
Oxbow			
14	0.053	67.02	0.0012
21	0.067	64.97	0.0015
22	0.042	65.26	0.0010

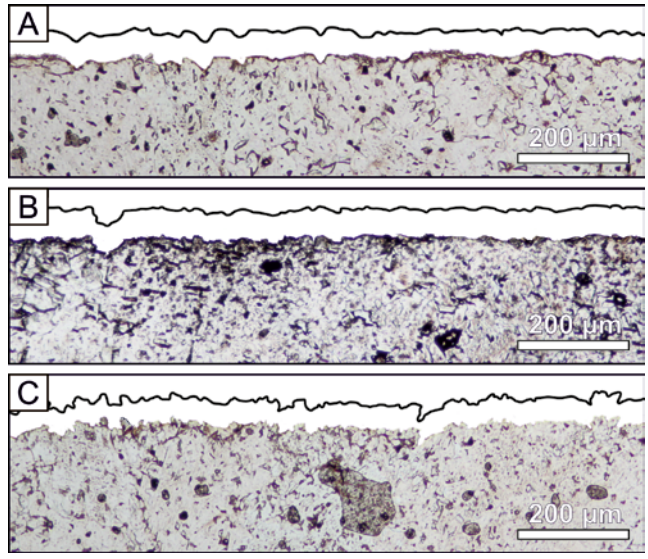

Fig. 2. Microtopographical differences between the experimental tablets. **A.** Surface of the experimental tablet, unexposed to corrosion. **B.** Surface of the experimental tablet, exposed to the interaction with a water in the oxbow. **C.** Surface of the experimental tablet, exposed to the interaction with river water. All photos were taken with parallel nicols. The lines were redrawn along the current surface of each plate to accentuate its microtopography.

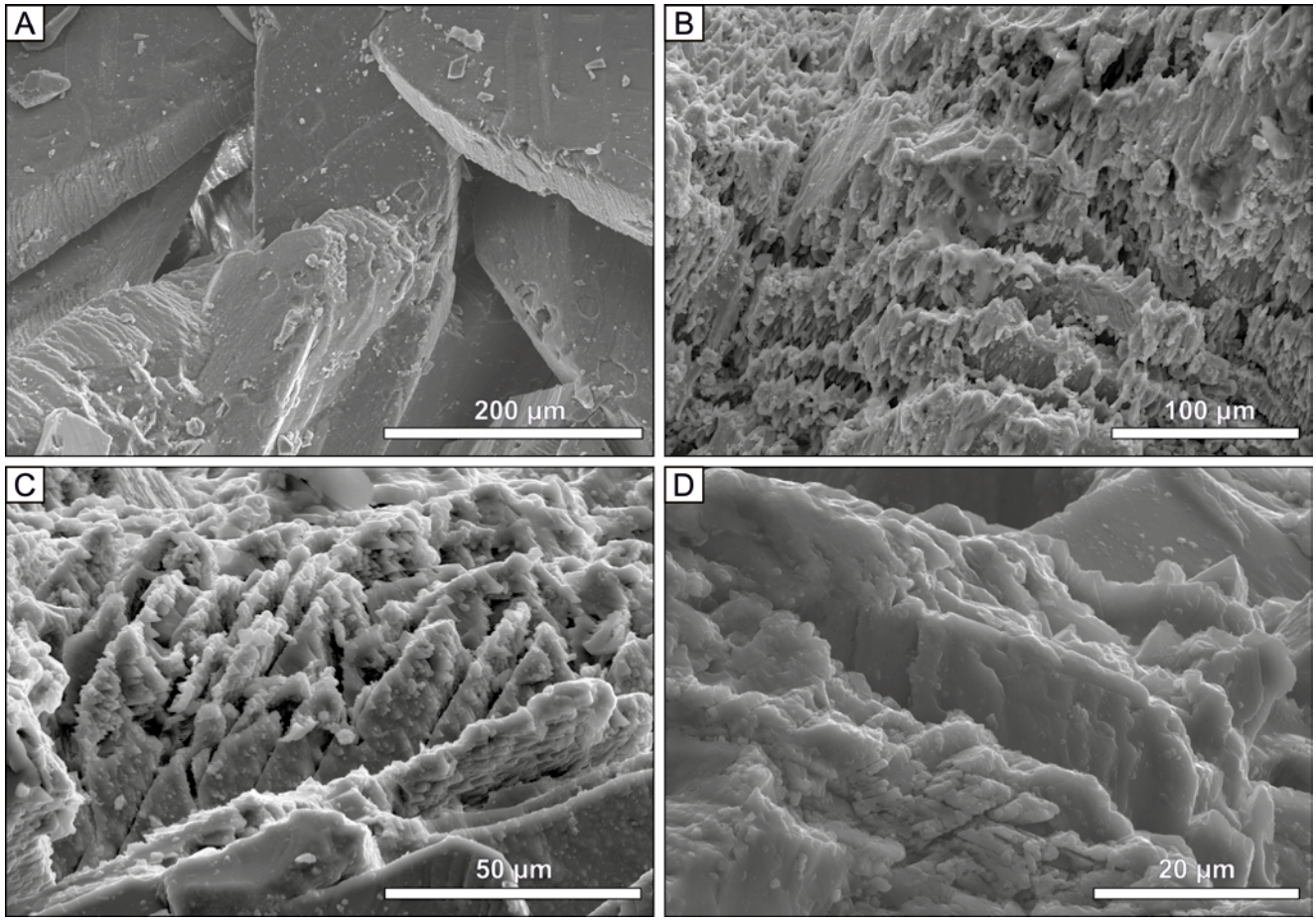

Fig. 3. Corrosion features developed in the experimental tablets. **A.** Calcite crystals in the tablet, not exposed to the erosion. **B.** The elongated dissolution pits and jagged face of calcite crystals that build the speleothem tablet, exposed for 908 days in the allogenic river. **C.** Dissolution features observed at the surface of experimental tablet, exposed for 908 days in the allogenic river. **D.** Small dissolution features developed at the surface of the experimental tablet, exposed for 908 days in the oxbow.

crystals are mostly well-rounded or flat, while their faces are considerably irregular and jagged. Noteworthy too is the fact that minor or no corrosion features were observed in some calcite crystals, covered by detrital sediments (Fig. 6C). This is most evident in the case of the spiky terminations of crystals that retained their original shape.

Although all the studied speleothem hiatuses show the presence of detrital sediments, their distribution and quantity can vary noticeably along the same layer (Figs 6D, 7A–D). The thickness usually ranges from less than 20 µm up to several millimetres. However, almost a 3-cm accumulation of detrital sediments was noted in the PD4 stalagmite. The detrital layers are mainly composed of quartz, biotite-muscovite, and clay minerals. In some cases, angular dolomite clasts were noted (Fig. 7B, D). The sizes of the detrital grains commonly ranged from a few micrometres to 0.2 mm and usually they are well-cemented by calcium carbonate.

The results of U-series dating of the hiatuses in the speleothems are presented in Table 4. These results show that

Table 4

Results of the U-series dating of the flowstones collected in the Prízemie Passage.

Sample no.	U cont. [ppm]	$^{234}U/^{238}U$	$^{230}Th/^{234}U$	$^{230}Th/^{232}Th$	Age [ka]	Corr. Age [ka]	Initial $^{234}U/^{238}U$
DMV1.1	1.102 ± 0.006	1.3923 ± 0.0029	0.6151 ± 0.0031	335.04 ± 1.6	98.72 ± 0.73		1.517 ± 0.012
DMV1.2	1.440 ± 0.009	1.4396 ± 0.0026	0.5139 ± 0.0023	130.95 ± 0.58	75.69 ± 0.46	75.04 ± 0.48	1.542 ± 0.011
DMV5.1	3.236 ± 0.022	0.8974 ± 0.0029	0.4843 ± 0.0049	539.9 ± 5.5	73.82 ± 1.05		0.874 ± 0.013
DMV5.2	9.674 ± 0.062	0.8646 ± 0.0011	0.4617 ± 0.0011	261.4 ± 0.65	69.34 ± 0.22	68.86 ± 0.25	0.836 ± 0.003

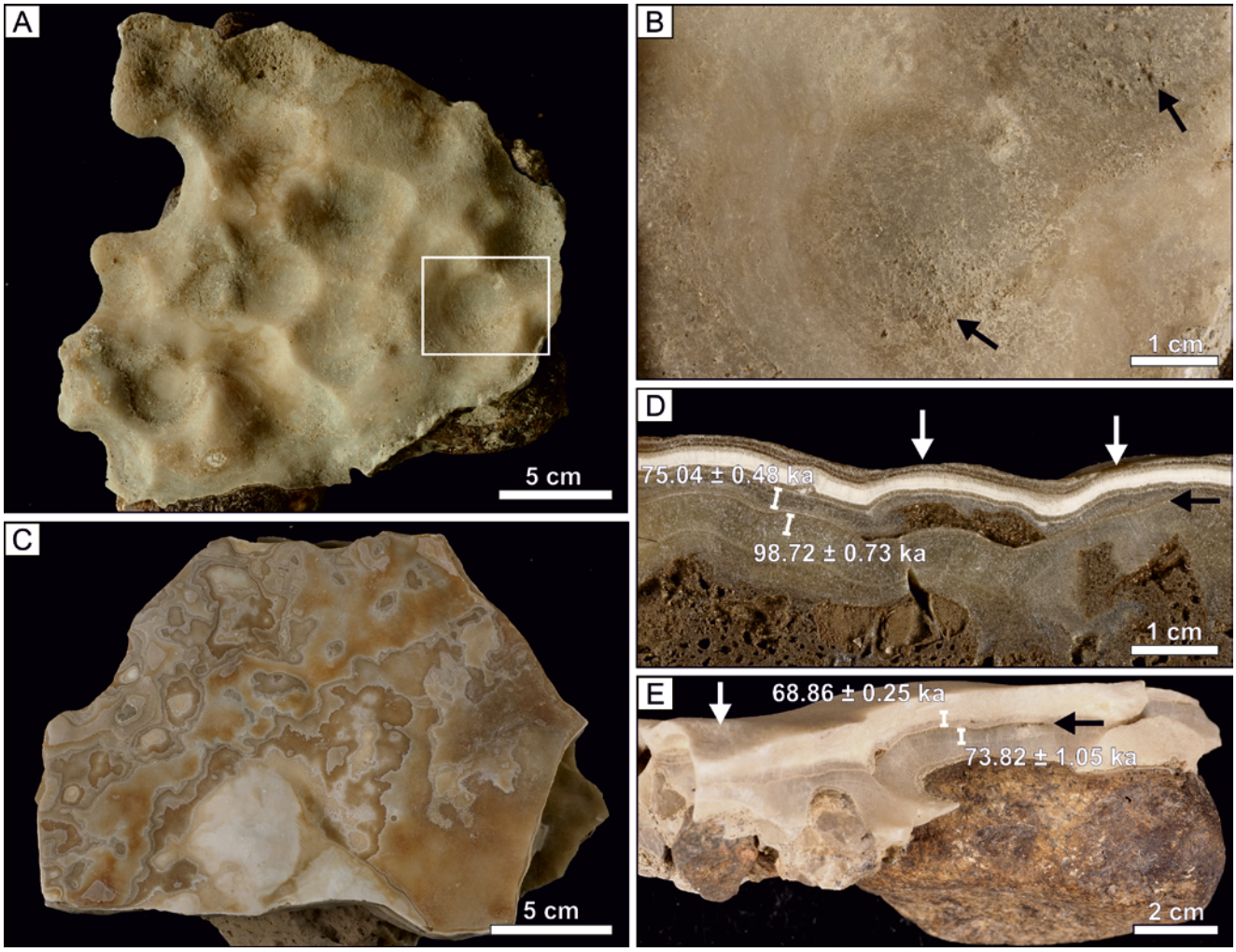

Fig. 4. Corrosion features developed owing to the interaction of flowstones with allogenic water. **A.** Scallops developed on the S10 flowstone surface. The frame indicates the area in B. **B.** Close-up view of the scallops. Arrows indicate small corrosion pits formed within the scallops. **C.** Irregularly corroded surface of the DMV1 flowstone. Mosaic-like appearance of the surface results from the unconformable exposure of the flowstone layers due to corrosion. **D.** Cross-section of the DMV1 flowstone. White arrows indicate truncations of the recent speleothem surface. Black arrow indicates the position of the growth hiatus within the flowstone. Brackets show the sampling position for U-series dating and its results. **E.** Cross-section of the DMV5 flowstone covering the granite and dolomite pebbles. Two subsequent phases of flowstone growth are separated by a thin siliciclastic layer. White arrow indicates the recent corrosion surface of the flowstone. Black arrow indicates the position of the growth hiatus within the flowstone. Brackets show the sampling position for U-series dating and its results.

the growth hiatuses within speleothems occurred between 98.72 ± 0.73 ka and 75.04 ± 0.48 ka (DMV1.1 and DMV1.2 subsamples, respectively; see also Fig. 4D), as well as between 73.82 ± 1.05 ka and 68.86 ± 0.25 ka (DMV5.1 and DMV5.2 subsamples, respectively; see also Fig. 4E). The renewal of speleothem growth usually is marked by the crystallization of chaotically arranged calcite crystals with a columnar microcrystalline fabric, showing competitive growth (Figs 6B, 7A, C). Such crystallization commonly was observed after a hiatus associated, with the presence of detrital sediments, tens of micrometres thick. On the other hand, the epitaxial overgrowths of calcite crystals after a hiatus were observed, where the detrital layer is discontinuous or does not exceed a thickness of 10 μm (Fig. 6D).

DISCUSSION

Rate of corrosion

The dissolution of speleothems, caused by an underground allogenic river, is indicated by the analyses of the pilot water samples. The calculated values of SI_{calc} range from –0.92 to –0.69 (Tab. 2). The dissolving capacity of these waters also is indicated by the weight loss of the speleothem tablets that ranged between 0.83 and 1.22 g, which corresponds to a dissolution rate of 0.018–0.029 mm/y (Tab. 3). These results are comparable with previous studies, based on experimental tablets placed in allogenic surficial streams that showed dissolution rates in the range of 0.10 to 0.14 mg $cm^{-2} \cdot d^{-1}$ (Hattanji *et al.*, 2014), which gives approximately 0.013 and 0.019 mm/y, respectively. A slightly

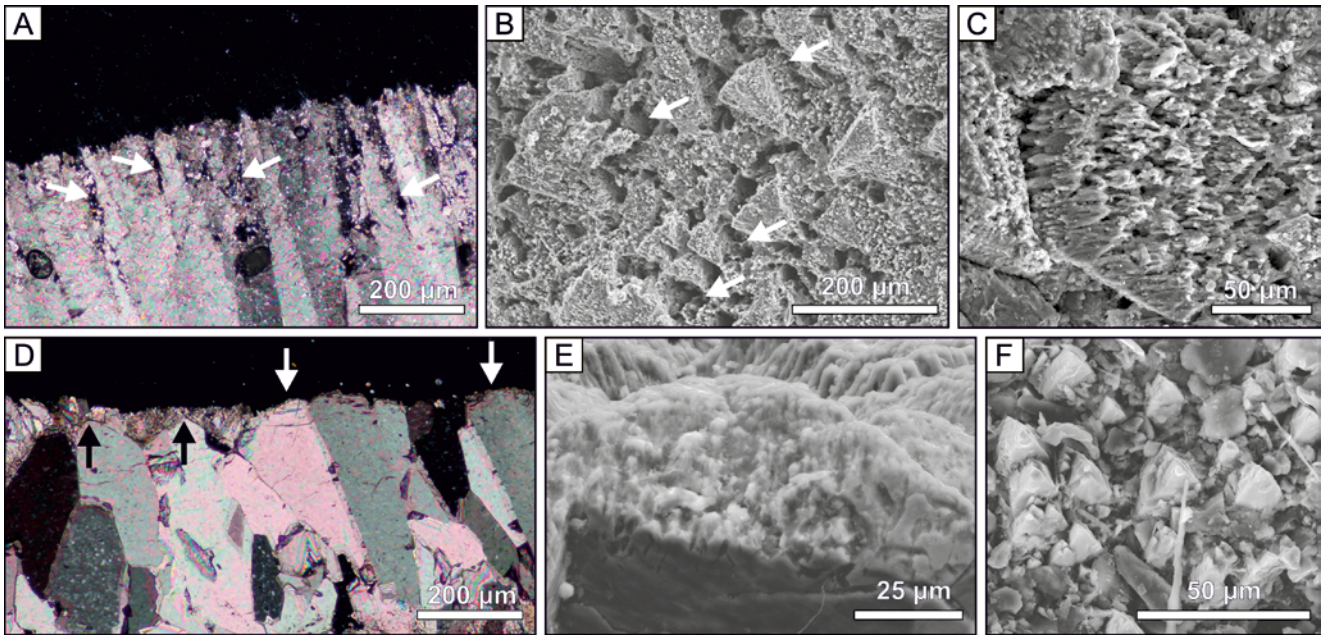

Fig. 5. Corrosion features developed on the surfaces of the speleothems. **A.** Corrosion pits (arrows) present at the junctions of calcite crystals, observed in thin section of the RA10 flowstone (microscopic image, crossed nicols). **B.** Corrosion pits (arrows) present between the calcite crystals, S1 flowstone surface (SEM image). **C.** Close-up view on the highly dissolved calcite crystals of the openwork structure in DMV1 flowstone (SEM image). **D.** Cross-section through the surface of the corroded DMV1 flowstone (microscopic image, crossed nicols). The original spiky terminations of calcite crystals (black arrows) retained under the overlying layer of flowstone, while those exposed to corrosion are well-rounded (white arrows). **E.** SEM image of well-rounded termination of the calcite crystal in the DMV1 flowstone. **F.** Calcite crystals of RA1 flowstone, which avoided corrosion, owing to being covered by the siliciclastic material.

higher average dissolution rate, up to 0.061 mm/y, was observed for the tablets installed in a ponor of Lekinka Cave in Slovenia, while tablets placed within the cave, 750 m downstream from ponor, had an average dissolution rate of up to 0.038 mm/y (Prelovšek, 2012). The river that enters Lekinka Cave partially flows through a marshy area; this indicates an increased input of biogenic CO_2 to the water, resulting in its increased aggressiveness towards carbonates. It can be assumed that the CO_2 input is the highest during warm seasons with dense vegetation cover, which can be indicated by the significant increase in the soil CO_2 concentrations in the warmer seasons (e.g., Spötl *et al.*, 2005; Baldini *et al.*, 2008; Frisia and Borsato, 2010). Therefore, during the warm seasons, allogenic rivers can be supplied, at least partially, with water containing more biogenic CO_2 drained from the local catchment area. Droppa (1996) documented the existence of seasonal variations in weight loss of the experimental tablets installed in a karst spring in the Demänová Valley, which showed higher weight loss during the summer (0.14 mm/y), thus in the period of increased vegetation, than in the winter (0.02 mm/y). This can support the hypothesis that an increased dissolution rate of carbonates occurs, owing to the higher input of biogenic CO_2.

The weight loss of the experimental tablets placed in the river contrasts with those in the oxbow, which is periodically supplied by the water of the Demänovka River that overflows the touristic path in the Prízemie Passage (Tab. 3). While the SI_{calc} of the pilot water samples from the oxbow shows only slightly higher values than in the case of the river (Tab. 2), the dissolution rate of the tablets differed considerably. Therefore, the present authors believe that the differences obtained cannot be explained solely by the chemical composition of these waters. The authors suggest that the dissolution rate of the experimental tablets was influenced by water motion. Within the flowing water, the diffusion boundary layer is disturbed by solution turbulence (Dreybrodt and Buhmann, 1991; Ford and Williams, 2007). Turbulent diffusion in such water can be responsible for the diffusion of potentially aggressive species through the diffusion boundary layer and their interaction with the carbonates (Dreybrodt and Buhmann, 1991; Ford and Williams, 2007). In contrast, in stagnant water, molecular diffusion predominates and therefore the ion exchange at the liquid-solid surface is limited. The minor dissolution of the tablets in the oxbow is explained by a sporadic increase in river discharge of the Demänovka River, which resulted in the infrequent and irregular supply of undersaturated water to the oxbow. This affected both the chemical composition of the oxbow water and the stagnant conditions, persisting in the oxbow.

One should consider that the abrasion, due to the sediment load carried by the river, also affected the total weight loss of the experimental tablets (Newson, 1971; Prelovšek, 2012; Wróblewski *et al.*, 2017; Blatnik *et al.*, 2020). In the Škocjanske Caves, the abrasion by sediment load was argued for a higher weight loss of the limestone tablets submerged in a river, but placed closer to the riverbed, than those installed higher in vertical profiles (Blatnik *et al.*, 2020). No studies on the volume of material carried by the Demänovka River have been conducted, so the authors cannot determine the effect of the abrasion process on the weight loss of the

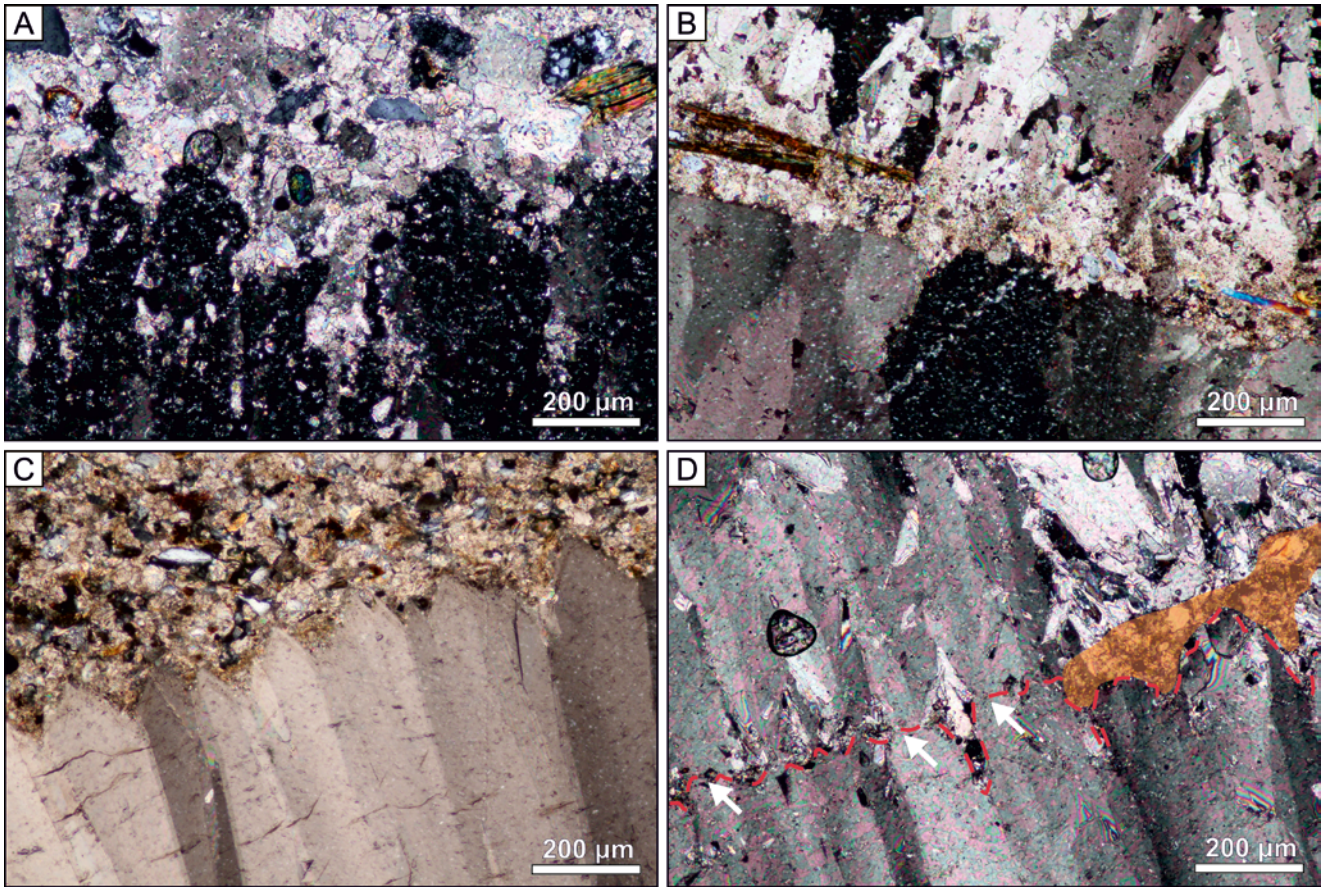

Fig. 6. Hiatuses resulting from the interaction of speleothems with an underground river. **A.** Clearly corroded calcite crystal below the hiatus in the RA10 flowstone. Note that some crystals have rounded terminations. **B.** Slightly corroded calcite crystal terminations, followed by a thin detrital layer in the DMV5 flowstone. **C.** Spiky termination of calcite crystals below the hiatus in the PD4 stalagmite. **D.** Lateral reduction of the detrital layer thickness (orange-shaded area) resulting in the epitaxial overgrowths of calcite crystals (arrows) in the RA10 flowstone. Red dashed line indicates the hiatus surface. All microscopic images were taken with crossed nicols.

experimental tablets. However, these tablets were placed behind limestone and speleothem blocks that acted as obstacles to the detrital particles, carried by the underground river (Fig. 1C). Therefore, the authors conclude that the abrasion of the tablets in this so-called shadow zone was negligible and therefore that the dissolution caused by the allogenic water was recognized as the dominant factor, responsible for the weight loss of the experimental tablets.

Features of speleothem hiatuses caused by allogenic rivers

Hiatuses within the speleothem sections commonly are identified by the presence of corroded calcite crystals and the non-carbonate mineral phases (e.g., Railsback *et al.*, 1994, 2013; Perrin *et al.*, 2014; Martín-Chivelet *et al.*, 2017; Tab. 5). Both of these can result from the dissolution of speleothems caused by allogenic water. A crucial factor that controls the dissolution of calcite crystals is the interaction time between speleothems and water undersaturated with respect to calcite. Owing to the short interaction time, the calcite crystals will most likely avoid significant dissolution (Fig. 6C). In this case, the calcite crystals should retain their original shapes (Tab. 5). This is the most evident in the crystals with the spiky terminations, which are potentially the most rapidly destroyed by the undersaturated water, carried by the allogenic rivers. Closer examination of the crystal faces can reveal the presence of a few tiny, initial corrosion pits, micrometres in diameter, which possibly were formed during the short interaction with aggressive water. As the interaction time increases, the initial corrosion pits within the calcite crystals widen and deepen. The authors assume that a moderate time of dissolution results in the development of corrosion pits that usually do not exceed tens of micrometres deep (Fig. 6B; Tab. 5). At this stage, the hiatus surfaces show some minor deviations in microtopography, relative to their original surface. This can be implied by the differences occurring in the microtopography of the experimental tablets (Fig. 2). As dissolution proceeded, the terminations of calcite crystals became more rounded, while their faces roughened. Finally, owing to the prolonged interaction of calcite crystals with aggressive water, dissolution leads to the formation of corrosion pits, up to hundreds of micrometres deep and some of them can be interconnected (Figs 5B, C, 6A; Tab. 5). Their presence is responsible for the development of the highly jagged microtopography of the hiatus surfaces. Prolonged dissolution of speleothems

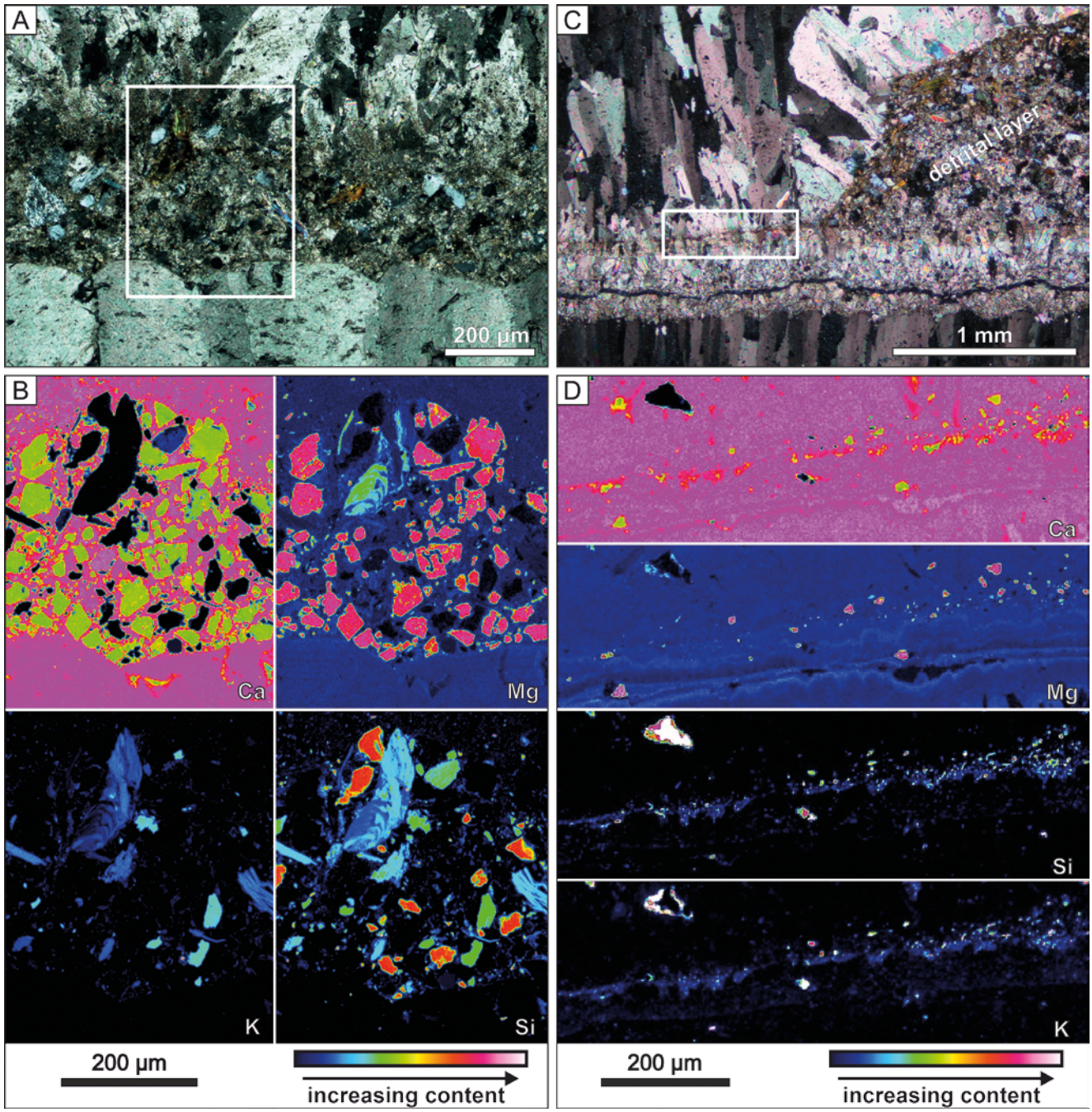

Fig. 7. Distribution and composition of the detrital material deposited by underground river and occurring within the speleothems. **A.** Detrital layer within the DMV5 flowstone (microscopic image, crossed nicols). Note that terminations of calcite crystals below the hiatus are flat or well-rounded. White frame indicates the area analysed in B. **B.** Distribution of the selected elements along the hiatus separating subsequent stages of the DMV5 flowstone growth (EMPA analyses). Numerous angular grains of dolomite are visible. **C.** Hiatus within the DMV1 flowstone (microscopic image, crossed nicols). Note that thickness of detrital layer decreases abruptly and continues only as a thin and discontinuous patches of siliciclastic material. White frame indicates the area analysed in D. **D.** Distribution of the selected elements along the hiatus within the DMV1 flowstone (EMPA analyses). Note that detrital material is highly scattered and mainly composed of fine-grained siliciclastics and individual dolomite grains.

can eventually produce macroscopically visible dissolution features. They are represented by the irregularly truncated surfaces (Fig. 4C, D), while scallops are the most definitive feature of the prolonged dissolution caused by aggressive allogenic water, carried by the underground river (Fig. 4A, B).

The authors suggest that the presence of the thick siliciclastic layer, deposited on speleothem surface by allogenic water, can impede the ion exchange reaction that occurs at the liquid-solid surface. Therefore, the overburden of siliciclastics hampers the dissolution of the speleothems that can occur owing to their interaction with aggressive water

Table 5

Hiatus features relative to the interaction time of speleothems with aggressive allogenic water and the deposition of detrital material, which controls the regrowth type of calcite crystals. Note that the regrowth type is not coupled with the various interaction time.

DISSOLUTION FEATURES		
Short interaction time	Moderate interaction time	Prolonged interaction time
Crystals terminations and faces mainly retain original structure Initial corrosion pits are formed	Corrosion pits are usually up to dozens of micrometres deep and wide Terminations of calcite crystals are slightly rounded Jagged hiatus surface	Scallops are common Corrosion pits are common and have diameters up to hundreds of micrometres Terminations of calcite crystals are well-rounded or flat Highly jagged hiatus surface is present
REGROWTH TYPE		
Scattered and fine-grained detrital material	Discontinuous layer or individual grains of detrital material	Continuous layers of detrital material
Epitaxial overgrowths of calcite crystals	Epitaxial overgrowths of calcite crystals are common Competitive growth of calcite crystals over the detrital material may occur	Competitive growth of calcite crystals over the detrital material

and demands an effective water exchange (Fig. 5F). For instance, the thick siliciclastic layer, observed within the PD4 stalagmite, may have contributed to the limited dissolution of the underlying calcite crystals (Fig. 6C).

Speleothem hiatuses, resulting from dissolution by the underground rivers, commonly are associated with the presence of detrital deposits. Detrital sediments, transported by allogenic rivers, usually are dominated by siliciclastics. However, this study documents that allogenic rivers also can transport reworked autochthonous material, i.e., dolomite grains. These grains finally were incorporated into speleothems (Fig. 7B, D). It should be noted that detrital grains also can be delivered to speleothems by dripwater or aeolian transport (Railsback *et al.*, 1999). The present authors suggest that the deposition of siliciclastic material by the underground river outpaced the aforementioned processes in both the number and size of grains. However, it should be noted that the uncemented sediments covering the speleothem can be removed later by river or drip water. In such a case, only the fine-grained and scattered siliciclastic material can evidence the interaction of the speleothem with an allogenic river that occurred in the past (Fig. 7C, D). If the detrital material has been significantly removed, the identification of the speleothem hiatuses that resulted from the interaction with aggressive river water also can be asserted from the presence of the dissolution features of the calcite crystals (Fig. 6D).

The deposition of detrital material on the speleothems is usually responsible for the interruption of calcite crystal growth. The renewal of calcite nucleation, due to the supply of drip water to a speleothem after a hiatus, can be followed by competitive crystal growth and can result in changes in the crystal fabric (Figs 6B, D, 7C; Tab. 5). These features are commonly present when the thickness of the detrital sediments exceeds tens of micrometres. On the other hand, the detrital layers the thickness of which does not exceed several micrometres, are followed by the epitaxial overgrowth of calcite crystals (Figs 6D, 7C; Tab. 5). This previously was observed by Perrin *et al.* (2014), who showed that detrital micro-layers occurring within stalagmites do not necessarily prevent the growth of the underlying crystals. Similar observations have been made for the detrital layers incorporated within a speleothem that resulted from floodwater deposition (González-Lemos *et al*., 2015b).

Relation between hiatuses and palaeoenvironmental conditions

Recent observations indicate that cave floodings are triggered by increased precipitation (e.g., Prelovšek, 2012; González-Lemos *et al.*, 2015a; Nannoni *et al.*, 2020). Extreme rainfall events have been indicated as responsible for the supply of detrital sediments, which in turn were incorporated into the speleothem structure (e.g., Finné *et al.*, 2014, 2015; Denniston *et al.*, 2015; González-Lemos *et al.*, 2015b; Denniston and Luetscher, 2017). Such events were apt to occur during the warm and humid interglacial conditions with increased amounts of precipitation. It can be speculated that at this time the allogenic water, which invaded the cave, had a higher aggressiveness towards carbonates, due to the increased uptake of soil CO_2 that followed the development of vegetation. Yet the corrosion features associated with the flood layers are rarely reported (González-Lemos *et al.,* 2015b). One can assume this is caused, owing to a short interaction time of speleothems with water undersaturated with respect to calcite, as in the case of some flowstones that have been taken from the section of the siliciclastic deposits

in the Prízemie Passage. Their growth interruptions were associated with the deposition of siliciclastics and occurred between ca 98.7 and 75.7 ka, as well as between 73.8 and 68.8 ka (Tab. 4; see also Fig. 4D, E). Considering the hydrological conditions in the Prízemie Passage at this time, it can be assumed that the speleothems that grew on the river sand bars were affected by the ephemeral flow of the water (Bella *et al.*, 2021). Under such conditions, the interaction of speleothems with allogenic water possibly occurred only during increased river drainage, forced by the intense rainfall, while the corrosion of speleothems was considerably limited.

It should be considered that the potential for speleothem dissolution in the past occurred during cave floods associated with deglaciation events. High rates of chemical weathering have been documented by studies on glacial meltwater quality (Brown, 2002). Fairchild *et al.* (1994, 1999) demonstrated that water within the proglacial streams and pools is undersaturated with respect to calcite. The corrosion of flowstones in Brestovská Cave during the late stage of MIS 2 was linked to the input of a large amount of water resulting from glacier thawing (Hercman *et al.,* 2008). Similar environmental conditions probably influenced the growth of the speleothems in the DCS, including the PD4 stalagmite the crystallization of which was interrupted by thick siliciclastic deposits. The hiatus in its growth ranges between 35 ± 0.25 and 15.5 ± 0.4 ka (Podgórska, 2019; Pawlak *et al.*, 2020). This hiatus resulted from (i) the harsh environmental conditions during the Last Glacial Maximum and prior to it and (ii) the deposition of the thick siliciclastic layer accumulated by the allogenic river. At this time, the burial of the stalagmite under a layer of allogenic sediments most likely was possible after the Last Glacial Maximum, probably between 20 and 16 ka, when deglaciation in the Carpathians had taken place (Makos *et al.,* 2014; Engel *et al.,* 2015). The study conducted in the Prízemie Passage shows that during this time the cave conduit was filled consecutively with siliciclastic deposits and was related to the higher water input that occurred during the deglaciation (Bella *et al*., 2021). However, the calcite crystals below the hiatus in the PD4 stalagmite yield only minor corrosion features, while their spiky terminations retained their original shape (Fig. 6C). This can indicate that the corrosion of the PD4 stalagmite by an allogenic river has not contributed considerably to the development of the hiatus. Negligible corrosion of calcite crystals possibly resulted from (i) the short interaction time of a speleothem with allogenic water or (ii) its reduced potential to dissolve carbonates. Considering the possibility of speleothem corrosion by glacial meltwater, the authors accept that the negligible corrosion of calcite crystals in the PD4 stalagmite was caused by their short interaction time with allogenic water. It can also be hypothesized that the PD4 stalagmite probably was rapidly buried by siliciclastic deposits, accumulating in a place of decreased river flow (i.e., a river bar), deposition of which was responsible for reducing speleothem corrosion (see above).

Finally, it should be underlined that the duration of the hiatuses is not reflected in the advancement of corrosion features. For instance, hiatuses that lasted over 20 ka noted in both PD4 stalagmite and DMV1 flowstone show only minor or no corrosion features (Figs 4D, 6C; Tab. 4). Conversely, a short hiatus (ca 5 ka) present within the DMV5 flowstone yields noticeable traces of corrosion (Figs 4E, 6B; Tab. 4). This indicates that the long hiatuses, detected within the speleothems, usually are not solely the result of their corrosion caused by allogenic rivers, even if its traces are present.

CONCLUSIONS

The interaction of speleothems with water, undersaturated with respect to calcite and carried by an allogenic river, results in their corrosion. The estimated dissolution rate, based on the weight loss of speleothem tablets, is up to 0.029 mm/y. This process depends mostly on speleothem-water interaction time and the chemical composition of the water. This interaction can shift to being more aggressive, owning to the supply of biogenic CO_2 that is favoured by the development of vegetation. Moreover, the overall dissolution rate possibly is influenced by the motion of the water and the deposition of siliciclastic sediments.

Prolonged dissolution of speleothems, caused by an allogenic river, is reflected in the development of corrosion pits and the degradation of both the terminations and faces of calcite crystals. On the other hand, in the case of a short interaction between speleothems and aggressive water, calcite crystals avoid significant corrosion and their original shapes can be preserved. For example, the episodes of interaction between speleothems and the allogenic river that occurred during the Vistulian (Weichselian) lack significant corrosion of calcite crystals. Regardless of the interaction time, corroded crystals are commonly covered with the siliciclastic sediments, the deposition of which determines the character of calcite crystallization after the growth hiatus. The overburden of speleothems by siliciclastic sediments, deposited by an underground river, also can limit the dissolution of underlying calcite crystals.

Acknowledgements

This study was financed by the National Science Centre of Poland (Project No. 2019/35/B/ST10/04397). We thank two anonymous reviewers for their useful comments and suggestions. We are grateful to Michał Gradziński and Wojciech Wróblewski for both their assistance during fieldwork and fruitful discussion that significantly improved the manuscript. We would like to acknowledge Irena Brunarska and Kinga Jarosz for their support with SEM analyses. We would like to appreciate the support of Adam Włodek during electron-microprobe analyses. Katarzyna Maj-Szeliga is thanked for the X-Ray diffraction measurements. The authors also thank Łukasz Jelonkiewicz for analyses of water samples.

REFERENCES

Baldini, J. U., McDermott, F., Hoffmann, D. L., Richards, D. A. & Clipson, N., 2008. Very high-frequency and seasonal cave atmosphere P_{CO2} variability: Implications for stalagmite growth and oxygen isotope-based paleoclimate records. *Earth and Planetary Science Letters*, 272: 118–129.

Bar-Matthews, M., Ayalon, A. & Kaufman, A., 1997. Late Quaternary paleoclimate in the eastern Mediterranean region from stable isotope analysis of speleothems at Soreq Cave, Israel. *Quaternary Research*, 47: 155–168.

Bar-Matthews, M., Marean, C. W., Jacobs, Z., Karkanas, P., Fisher, E. C., Herries, A. I., Brown, K., Williams H. M., Bernatchez, J., Ayalon, A. & Nilssen, P. J., 2010. A high resolution and continuous isotopic speleothem record of paleoclimate and paleoenvironment from 90 to 53 ka from Pinnacle Point on the south coast of South Africa. *Quaternary Science Reviews*, 29: 2131–2145.

Bella, P., Gradziński, M., Hercman, H., Leszczyński, S. & Nemec, W., 2021. Sedimentary anatomy and hydrological record of relic fluvial deposits in a karst cave conduit. *Sedimentology*, 68: 425–448.

Bella, P., Haviarová, D., Kováč, Ľ., Lalkovič, M., Sabol, M., Soják, M., Struhár, V., Višňovská, Z. & Zelinka, J., 2014. *Caves of the Demänova Valley.* Štátna Ochrana Prírody Slovenskej Republiky, Správa Slovenských Jaskýň, Liptovský Mikuláš, 200 pp. [In Slovak, with English summary.]

Bernal-Wormull, J. L., Moreno, A., Bartolomé, M., Arriolabengoa, M., Pérez-Mejías, C., Iriarte, E., Osácar, C., Spötl, C., Stoll, H., Cacho, I., Edwards, R. L. & Cheng, H., 2023. New insights into the climate of northern Iberia during the Younger Dryas and Holocene: The Mendukilo multi-speleothem record. *Quaternary Science Reviews*, 305: 108006.

Biely, A., Beňuška, P., Bezák, V., Bujnovský, A., Halouzka, R., Ivanička, J., Kohút, M., Klinec, A., Lukáčik, E., Maglay, J., Miko, O., Pulec, M., Putiš, M. & Vozár, J., 1992. *Geological Map of the Nízke Tatry Mountains 1: 50 000*. Geologický ústav Dionýza Štúra, Bratislava.

Blatnik, M., Culver, D. C., Gabrovšek, F., Knez, M., Kogovšek, B., Kogovšek, J., Liu, H., Mayaud, C., Mihevc, A., Mulec, J., Năpăruş-Aljančič, M., Otoničar, B., Petrič, M., Pipan, T., Prelovšek, M., Ravbar, N., Shaw, T., Slabe, T., Šebela, S. & Zupan Hajna N., 2020. Measurements of present-day limestone dissolution and calcite recipitation rates with limestone tablets in stream caves (with the case study of Škocjanske Jame). In: Knez, M., Otoničar, B., Petrič, M., Pipan, T. & Slabe, T. (eds), *Karstology in the Classical Karst. Advances in Karst Science.* Springer, Cham, pp. 115–126.

Błaszczyk, M. & Hercman, H., 2022. Palaeoclimate in the Low Tatras of the Western Carpathians during MIS 11–6: Insights from multiproxy speleothem records. *Quaternary Science Reviews*, 275: 107290.

Bosák, P., Hercman, H., Mihevc, A. & Pruner, P., 2002. High resolution magnetostratigraphy of speleothems from Snežna Jama, Kamniške-Savinja Alps, Slovenia. *Acta Carsologica*, 31: 15–32.

Brown, G. H., 2002. Glacier meltwater hydrochemistry. *Applied Geochemistry*, 17: 855–883.

Burns, S. J., Fleitmann, D., Matter, A., Neff, U. & Mangini, A., 2001. Speleothem evidence from Oman for continental pluvial events during interglacial periods. *Geology*, 29: 623–626.

Cruz, F. W., Jr., Burns, S. J., Jercinovic, M., Karmann, I., Sharp, W. D. & Vuille, M., 2007. Evidence of rainfall variations in Southern Brazil from trace element ratios (Mg/Ca and Sr/Ca) in a Late Pleistocene stalagmite. *Geochimica et Cosmochimica Acta*, 71: 2250–2263.

Cruz, F. W., Jr., Burns, S. J., Karmann, I., Sharp, W. D., Vuille, M., Cardoso, A. O., Ferrari, J. A., Silva Dias, P. L. & Viana, O., Jr., 2005. Insolation-driven changes in atmospheric circulation over the past 116,000 years in subtropical Brazil. *Nature*, 434: 63–66.

Dasgupta, S., Saar, M. O., Edwards, R. L., Shen, C. C., Cheng, H. & Alexander, E. C., Jr., 2010. Three thousand years of extreme rainfall events recorded in stalagmites from Spring Valley Caverns, Minnesota. *Earth and Planetary Science Letters*, 300: 46–54.

Denniston, R. F. & Luetscher, M., 2017. Speleothems as high-resolution paleoflood archives. *Quaternary Science Reviews*, 170: 1–13.

Denniston, R. F., Villarini, G., Gonzales, A. N., Wyrwoll, K. H., Polyak, V. J., Ummenhofer, C. C., Lachniet, M. S., Wanamaker, A. D., Jr., Humphreys, W. F., Woods, D. & Cugley, J., 2015. Extreme rainfall activity in the Australian tropics reflects changes in the El Niño/Southern Oscillation over the last two millennia. *Proceedings of the National Academy of Sciences*, 112: 4576–4581.

Dorale, J. A., Lepley, S. W. & Edwards, R. L., 2005. The ultimate flood recorder: flood deposited sediments preserved in stalagmites. *Geophysical Research Abstracts*, 7: 09901.

Dreybrodt, W. & Buhmann, D., 1991. A mass transfer model for dissolution and precipitation of calcite from solutions in turbulent motion. *Chemical Geology*, 90: 107–122.

Droppa, A., 1957. *Die Höhlen Demänovské Jaskyne.* SAV, Bratislava, 289 pp. [In Slovak, with German summary.]

Droppa, A., 1966. The correlation of some horizontal caves with river terraces. *Studies in Speleology*, 1: 186–192.

Droppa, A., 1972. Die geomorphologischen Verhältniosse im Demänovská-Tal. *Slovenský Kras*, 10: 9–46. [In Slovak, with German abstract.]

Droppa, A., 1996. Vplyv ročných období na koróziu Demänovského krasu. In: Lalkovič, M. (ed.), *Kras a jaskyne – výskum, využívanie a ochrana, Liptovský Mikuláš, October 10–11, 1995. Zborník referátov z vedeckej konferencie*. SMOPaJ, Liptovský Mikuláš, pp. 63–70. [In Slovak, with English summary]

Engel, Z., Mentlík, P., Braucher, R., Minár, J., Léanni, L. & Aster Team, 2015. Geomorphological evidence and ^{10}Be exposure ages for the Last Glacial Maximum and deglaciation of the Velká and Malá Studená dolina valleys in the High Tatra Mountains, central Europe. *Quaternary Science Reviews*, 124: 106–123.

Fairchild, I. J. & Baker, A., 2012. *Speleothem Science: From Process to Past Environments*. John Wiley & Sons, Oxford, 432 pp.

Fairchild, I. J., Bradby, L., Sharp, M. & Tison, J. L., 1994. Hydrochemistry of carbonate terrains in alpine glacial settings. *Earth Surface Processes and Landforms*, 19: 33–54.

Fairchild, I. J., Killawee, J. A., Hubbard, B. & Dreybrodt, W., 1999. Interactions of calcareous suspended sediment with glacial meltwater: a field test of dissolution behaviour. *Chemical Geology*, 155: 243–263.

Feinberg, J. M., Lascu, I., Lima, E. A., Weiss, B. P., Dorale, J. A., Alexander, E. C., Jr. & Edwards, R. L., 2020. Magnetic detection of paleoflood layers in stalagmites and implications for historical land use changes. *Earth and Planetary Science Letters*, 530: 115946.

Finné, M., Bar-Matthews, M., Holmgren, K., Sundqvist, H. S., Liakopoulos, I. & Zhang, Q., 2014. Speleothem evidence for late Holocene climate variability and floods in Southern Greece. *Quaternary Research*, 81: 213–227.

Finné, M., Kylander, M., Boyd, M., Sundqvist, H. S. & Löwemark, L., 2015. Can XRF scanning of speleothems be used as a non-destructive method to identify paleoflood events in caves? *International Journal of Speleology*, 44: 17–23.

Ford, D. C. & Williams, P. W., 2007. *Karst Geomorphology and Hydrology*. John Wiley & Sons, London, 562 pp.

Frisia S., 2015. Microstratigraphic logging of calcite fabrics in speleothems as tool for palaeoclimate studies. *International Journal of Speleology*, 44: 1–16.

Frisia, S. & Borsato, A., 2010. Karst. In: Alonso-Zarza, A. M. & Tanner, L. H. (eds), *Carbonates in Continental Settings: Facies, Environments, and Processes. Developments in Sedimentology*, 61: 269–318.

Frumkin, A., Carmi, I., Gopher, A., Ford, D. C., Schwarcz, H. P. & Tsuk, T., 1999. A Holocene millennial-scale climatic cycle from a speleothem in Nahal Qanah Cave, Israel. *The Holocene*, 9: 677–682.

Gaál, Ľ., 2016. Lithology of carbonate rocks of Demänová Cave System. *Slovenský Kras*, 54: 109–129. [In Slovak, with English summary.]

Gaál, Ľ. & Michalík, J., 2017. Middle Triassic limestones in the Okno Cave (Demänovská dolina Valley, Low Tatras): lithology and facies types. *Slovenský Kras*, 55: 145–154. [In Slovak, with English summary.]

Gázquez, F., Calaforra, J. M., Forti, P., Stoll, H., Ghaleb, B. & Delgado-Huertas, A., 2014. Paleoflood events recorded by speleothems in caves. *Earth Surface Processes and Landforms*, 39: 1345–1353.

González-Lemos, S., Jiménez-Sánchez, M. & Stoll, H. M., 2015a. Sediment transport during recent cave flooding events and characterization of speleothem archives of past flooding. *Geomorphology*, 228: 87–100.

González-Lemos, S., Müller, W., Pisonero, J., Cheng, H., Edwards, R. L. & Stoll, H. M., 2015b. Holocene flood frequency reconstruction from speleothems in northern Spain. *Quaternary Science Reviews*, 127: 129–140.

Hattanji, T., Ueda, M., Song, W., Ishii, N., Hayakawa, Y. S., Takaya, Y. & Matsukura, Y., 2014. Field and laboratory experiments on high dissolution rates of limestone in stream flow. *Geomorphology*, 204: 485–492.

Haviarová, D., Gradziński, M. & Motyka, J., 2021. Chemical composition of water in the Demänová Cave of Liberty (Demänovská dolina Valley, Nízke Tatry Mts.) *Slovenský Kras*, 59: 157–186. [In Slovak, with English summary.]

Hellstrom, J., 2003. Rapid and accurate U/Th dating using parallel ion counting multicollector ICP-MS. *Journal of Analytical Atomic Spectrometry*, 18: 1346–1351.

Hellstrom, J., 2006. U-Th dating of speleothems with high initial ^{230}Th using stratigraphical constraint. *Quaternary Geochronology*, 1: 289–295.

Hercman, H., 2000. Reconstruction of palaeoclimatic changes in central Europe between 10 and 200 thousand years BP, based on analysis of growth frequency of speleothems. *Studia Quaternaria*, 17: 35–70.

Hercman, H., Gąsiorowski, M., Szczygieł, J., Bella, P., Gradziński, M., Błaszczyk, M., Matoušková, Š., Pruner, P. & Bosák, P., 2023. Delayed valley incision due to karst capture (Demänová Cave System, Western Carpathians, Slovakia). *Geomorphology*, 437: 108809.

Hercman, H., Gradziński, M. & Bella, P., 2008. Evolution of Brestovská Cave based on U-series dating of speleothems. *Geochronometria*, 32: 1–12.

Kagan, E. J., Agnon, A., Bar-Matthews, M. & Ayalon, A., 2005. Dating large infrequent earthquakes by damaged cave deposits. *Geology*, 33: 261–264.

Krklec, K., Domínguez-Villar, D. & Perica, D., 2021. Use of rock tablet method to measure rock weathering and landscape denudation. *Earth-Science Reviews*, 212: 103449.

Louček, D., Michovská, J. & Trefná, E., 1960. Glaciation of the Low Tatra Mountains. *Sborník Československé Společnosti Zeměpisné*, 65: 326–352. [In Czech, with English summary.]

Makos, M., Dzierżek, J., Nitychoruk, J. & Zreda, M., 2014. Timing of glacier advances and climate in the High Tatra Mountains (Western Carpathians) during the Last Glacial Maximum. *Quaternary Research*, 82: 1–13.

Martín-Chivelet, J., Muñoz-García, M. B., Cruz, J. A., Ortega, A. I. & Turrero, M. J., 2017. Speleothem Architectural Analysis: Integrated approach for stalagmite-based paleoclimate research. *Sedimentary Geology*, 353: 28–45.

Moreno, A., Stoll, H., Jiménez-Sánchez, M., Cacho, I., Valero-Garcés, B., Ito, E. & Edwards, R. L., 2010. A speleothem record of glacial (25–11.6 kyr BP) rapid climatic changes from northern Iberian Peninsula. *Global and Planetary Change*, 71: 218–231.

Motyka, J., Gradziński, M., Bella, P. & Holúbek, P., 2005. Chemistry of waters from selected caves in Slovakia – a reconnaissance study. *Environmental Geology*, 48: 682–692.

Nannoni, A., Vigna, B., Fiorucci, A., Antonellini, M. & De Waele, J., 2020. Effects of an extreme flood event on an alpine karst system. *Journal of Hydrology*, 590: 125493.

Newson, M. D., 1971. The role of abrasion in cavern development. *Cave Research Group of Great Britain, Transactions*, 13: 101–107.

Palmer, A. N., 2001. Dynamics of cave development by allogenic water. *Acta Carsologica*, 30: 13–32.

Parkhurst, D. L. & Appelo, C. A. J., 2013. *Description of Input and Examples for PHREEQC Version 3 – A Computer Program for Speciation, Batch-Reaction, One-Dimensional Transport, and Inverse Geochemical Calculations. U.S. Geological Survey Techniques and Methods, Book 6, Chap. A43*. U.S Geological Survey, Denver, Colorado, 497 pp.

Pawlak, J., Hercman, H., Sierpień, P., Pruner, P., Gąsiorowski, M., Mihevc, A., Zupan Hajna, N., Bosák, P., Błaszczyk, M. & Wach, B., 2020. Estimation of the durations of breaks in deposition – Speleothem case study. *Geochronometria*, 47: 154–170.

Perrin, C., Prestimonaco, L., Servelle, G., Tilhac, R., Maury, M. & Cabrol, P., 2014. Aragonite-calcite speleothems: identifying original and diagenetic features. *Journal of Sedimentary Research*, 84: 245–269.

Plagnes, V., Causse, C., Genty, D., Paterne, M. & Blamart, D., 2002. A discontinuous climatic record from 187 to 74 ka from a speleothem of the Clamouse Cave (south of France). *Earth and Planetary Science Letters*, 201: 87–103.

Podgórska, D., 2019. *Reconstruction of Vistulian Palaeoenvironmental Conditions Based on Analysis of Speleothems from the Demänová Cave System*. Unpublished PhD Thesis, Jagiellonian University, Kraków, 116 pp. [In Polish, with English summary.]

Prelovšek, M., 2012. *The Dynamics of Present-Day Speleogenetic Processes in the Stream Caves of Slovenia*. Založba ZRC, Ljubljana, 152 pp.

Quigley, M. C., Horton, T., Hellstrom, J. C., Cupper, M. L. & Sandiford, M., 2010. Holocene climate change in arid Australia from speleothem and alluvial records. *The Holocene*, 20: 1093–1104.

Railsback, L. B., Akers, P. D., Wang, L., Holdridge, G. A. & Voarintsoa, N. R., 2013. Layer-bounding surfaces in stalagmites as keys to better paleoclimatological histories and chronologies. *International Journal of Speleology*, 42: 167–180.

Railsback, L. B., Brook, G. A., Chen, J., Kalin, R. & Fleisher, C. J., 1994. Environmental controls on the petrology of a late Holocene speleothem from Botswana with annual layers of aragonite and calcite. *Journal of Sedimentary Research*, 64: 147–155.

Railsback, L. B., Brook, G. A. & Webster, J. W., 1999. Petrology and paleoenvironmental significance of detrital sand and silt in a stalagmite from Drotsky's Cave, Botswana. *Physical Geography*, 20: 331–347.

Sala, P., Bella, P., Szczygieł, J., Wróblewski, W. & Gradziński, M., 2022. Healed speleothems: A possible indicator of seismotectonic activity in karst areas. *Sedimentary Geology*, 430: 106105.

Sánchez-Moreno, E. M., Font, E., Pavón-Carrasco, F. J., Dimuccio, L. A., Hillaire-Marcel, C., Ghaleb, B. & Cunha, L., 2022. Paleomagnetic techniques can date speleothems with high concentrations of detrital material. *Scientific Reports*, 12: 17936.

Sierpień, P., Bosák, P., Hercman, H., Pawlak, J., Pruner, P., Zupan Hajna, N. & Mihevc, A., 2021. Flowstones from the Račiška Pečina Cave (SW Slovenia) record 3.2-Ma-long history. *Geochronometria*, 48: 31–45.

Spötl, C., Fairchild, I. J. & Tooth, A. F., 2005. Cave air control on dripwater geochemistry, Obir Caves (Austria): Implications for speleothem deposition in dynamically ventilated caves. *Geochimica et Cosmochimica Acta*, 69: 2451–2468.

Spötl, C., Mangini, A. & Richards, D. A., 2006. Chronology and paleoenvironment of Marine Isotope Stage 3 from two high-elevation speleothems, Austrian Alps. *Quaternary Science Reviews*, 25: 1127–1136.

Szczygieł, J., Gradziński, M., Bella, P., Hercman, H., Littva, J., Mendecki, M. J., Sala, P. & Wróblewski, W., 2021. Quaternary faulting in the Western Carpathians: Insights into paleoseismology from cave deformations and damaged speleothems (Demänová Cave System, Low Tatra Mts). *Tectonophysics*, 820: 229111.

Vitásek, F., 1923. Plistocaen dans la vallée de la Demänová (Slovaquie). *Sborník Státního geologického ústavu Československé republiky*, 2: 157–171. [In Czech, with French summary.]

Warken, S. F., Fohlmeister, J., Schröder-Ritzrau, A., Constantin, S., Spötl, C., Gerdes, A., Esper, J., Frank, N., Arps, J., Terente, M., Riechelmann, D. F. C., Mangini, A. & Scholz, D., 2018. Reconstruction of late Holocene autumn/winter precipitation variability in SW Romania from a high-resolution speleothem trace element record. *Earth and Planetary Science Letters*, 499: 122–133.

Wróblewski, W., Gradziński, M., Motyka, J. & Stankovič, J., 2017. Recently growing subaqueous flowstones: Occurrence, petrography, and growth conditions. *Quaternary International*, 437: 84–97.

Zupan Hajna, N., Mihevc, A., Bosák, P., Pruner, P., Hercman, H., Horáček, I., Wagner, J., Čermák, J., Pawlak, J., Sierpień, P., Kdýr, Š., Juřičková, L. & Švara, A., 2021. Pliocene to Holocene chronostratigraphy and paleoenvironmental records from cave sediments: Račiška pečina section (SW Slovenia). *Quaternary International*, 605–606: 5–24.